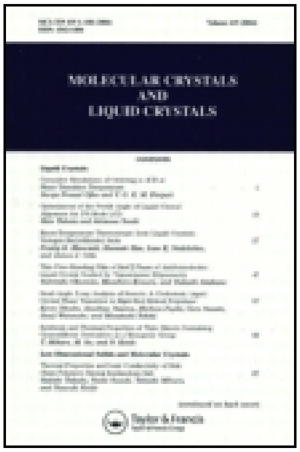

Molecular Crystals and Liquid Crystals Science and Technology. Section A. Molecular Crystals and Liquid Crystals
Publication details, including instructions for authors and subscription information:
http://www.tandfonline.com/loi/gmcl19

Spacer Length Dependence of Tilt Angle of Mesogenic Chromophores of Side-Chain Liquid-Crystalline Polysiloxanes

Makoto Hasegawa [a], Nobukatso Nemoto [b], Yu Nagase [b], Yasuo Shirai [c], Jiro Abe [c] & Tomiki Ikeda [a]

[a] Research Laboratory of Resource Utilization, Tokyo Institute of Technology, 4259 Nagatsuta, Midori-ku, Yokohama, 227, Japan

[b] Sagami Chemical Research Center, 4-4-1 Nishi-Ohnuma, Sagamihara, Kanagawa, 229, Japan

[c] Department of Photo-Optical Engineering, Faculty of Engineering, Tokyo Institute of Polytechnics, 1583 Iiyama, Atsugi, Kanagawa, 243-02, Japan

To cite this article: Makoto Hasegawa, Nobukatso Nemoto, Yu Nagase, Yasuo Shirai, Jiro Abe & Tomiki Ikeda (1998): Spacer Length Dependence of Tilt Angle of Mesogenic Chromophores of Side-Chain Liquid-Crystalline Polysiloxanes, Molecular Crystals and Liquid Crystals Science and Technology. Section A. Molecular Crystals and Liquid Crystals, 318:1, 71-86

To link to this article: http://dx.doi.org/10.1080/10587259808045376

Mol. Cryst. Liq. Cryst., Vol. 318, pp. 71-86
Reprints available directly from the publisher
Photocopying permitted by license only

Spacer Length Dependence of Tilt Angle of Mesogenic Chromophores of Side-Chain Liquid-Crystalline Polysiloxanes

MAKOTO HASEGAWA[a], NOBUKATSU NEMOTO[b], YU NAGASE[b], YASUO SHIRAI[c], JIRO ABE[c] and TOMIKI IKEDA*[a]
[a]Research Laboratory of Resource Utilization, Tokyo Institute of Technology, 4259 Nagatsuta, Midori-ku, Yokohama 227, Japan; [b]Sagami Chemical Research Center, 4-4-1 Nishi-Ohnuma, Sagamihara, Kanagawa 229, Japan; [c]Department of Photo-Optical Engineering, Faculty of Engineering, Tokyo Institute of Polytechnics, 1583 Iiyama, Atsugi, Kanagawa 243-02, Japan

The orientational behavior for a series of side-chain liquid-crystalline polysiloxanes incorporating azo chromophores, i.e., poly(3-{4-[(4-nitrophenyl)azo]phenyl]oxycarbonyl}propylmethylsiloxane)-co-(3-carboxypropylmethylsiloxane) (**P1**), poly{3-[(6-{[4-[(4-nitrophenyl)azo]phenyl]oxy}hexyl)oxycarbonyl]propylmethylsiloxane}-co-(3-carboxypropylmethylsiloxane) (**P2**), and poly{3-[(11-{[4-[(4-nitrophenyl)azo]phenyl]oxy}undecyl)oxycarbonyl]propylmethylsiloxane}-co-(3-carboxypropylmethylsiloxane) (**P3**) were investigated by UV-Vis and polarized FTIR-ATR spectroscopy as well as X-ray diffraction measurement using their thin films. **P1** exhibited highly-ordered smectic and nematic phases as the mesophases. On the other hand, **P2** and **P3** showed only smectic C phase. The mesogenic chromophores of these polymers in smectic phases and the once-annealed solid were spontaneously aligned nearly normal to a substrate surface. In the case of **P1**, the tilt angle of the mesogenic chromophores in the nematic phase was found to be larger than that in the smectic phase. The tilt angles of the mesogenic chromophores of these polymers in the smectic phase and in the once-annealed solid increased with the increase in the side-chain methylene spacer units. The dependence of the tilt angle on the spacer length was concluded to be attributable to the changes in intermolecular interactions with relation to the degree of the motion decoupling between the side-chain and main-chain.

Keywords: liquid-crystalline polysiloxane; flexible spacer; tilt angle; electrical intermolecular interactions

INTRODUCTION

Side-chain liquid-crystalline polymers (SLCPs) exhibit the properties of low-molecular-weight liquid crystals (LMWLCs) as well as those of polymers[1-3]. Therefore, SLCPs are applicable in electro-optical and all-optical materials as conventional LMWLCs[4-6]. It has been pointed out that the effect of flexible spacer length is an important factor in technological points of view as well as scientific standpoints. The flexible spacer in SLCPs plays an important roles in its plasticizing effect and stabilization of the mesophase due to the decoupling of the motion between the side chain and the main chain[7-12]. Moreover, the flexible spacer affect the packing manner and the morphology in state of aggregation. There have been many reports with relation to the effects of the flexible spacer on liquid-crystalline properties[13-18]. However, little study for the relation between the spacer length and the tilt angle of the mesogenic chromophores against the layer plane in smectic phase has been reported.

In our previous papers, the behavior of the electric-field-induced dipolar alignment of mesogenic chromophores with the thin film of the side-chain liquid-crystalline polysiloxane containing mesogenic NLO-active azo chromophores was investigated[19-20]. This polymer, i.e., **P2** which has six methylene units between side-chain carbonyl and phenoxy groups, exhibits a smectic C liquid-crystalline phase in the temperature range from 59 to 113 °C. From the spectroscopic analyses, it was found that the mesogenic chromophores of **P2** aligned almost perpendicular to a substrate surface in the crystalline and smectic C phases. Moreover, the mesogenic chromophores of **P2** formed the interdigited alignment in the crystalline and smectic C phases. In addition, we also prepared analogous, i.e., **P1** and **P3** which have no and eleven methylene units between the side-chain carbonyl and phenoxy groups, respectively, and performed the identification of the mesophases.

In this paper, the relationship between the methylene spacer length and the tilt angle of the mesogenic chromophores of the present series for the side-chain liquid-crystalline polysiloxanes was investigated by UV-Vis, FTIR-ATR spectroscopies and X-ray diffraction measurements.

EXPERIMENTS

Materials

Details of the preparation of **P1-3** were described in our previous report[19]. The structure of these polymers are shown in Figure 1. The general properties of **P1-3** are summarized in Table I.

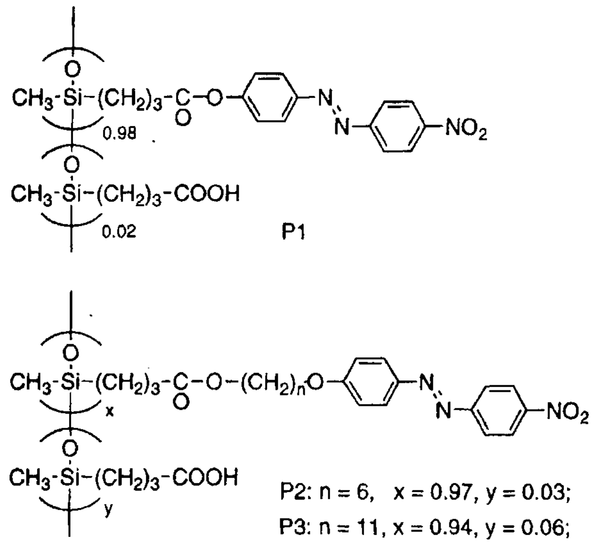

FIGURE 1 Structure of polymer **P1**, **P2** and **P3**.

Film Preparation

Polymer films (~1 μm thick) were prepared by spin coating from a 5 wt % THF solution of each polymer at a rate of 2000 rpm. These solutions were passed through a 0.50 μm filter (Millipore)to remove particle impurities before spin coating. These spin-coated samples were placed in a vacuum oven at ~30 °C for over 24 h to obtain solvent-free films.

TABLE I Molecular weights and thermal properties of **P1-3**

Polymer	$M_n \times 10^{-3}$ [a]	M_w / M_n [b]	T_g (°C)	Phase transitions[c] (°C)
1	2.06	1.45	12	K 68 Sx 97 N 148 I
2	2.43	1.75	-19	K 59 Sc 113 I
3	45.9	3.82	15	K 49 Sc 118 I

[a] Determined by GPC using a polystyrene-calibrated column set. [b] Polydispersity index. [c] Determined from DSC measurements, polarized microscopic observation, and X-ray diffraction measurements.

RESULTS AND DISCUSSION

Polarized FTIR-ATR Spectroscopy

These liquid-crystalline polysiloxanes show two kinds of solid states in film. One is received for the as-cast film (solid **B**), and the other state is obtained for the once-annealed film (solid **A**), which can be obtained by heating the as-cast film to the mesophase temperature. In order to investigate the alignment of the mesogenic chromophores against a substrate surface in those states, polarized FTIR-ATR spectra were measured. Figures 2-4 show the polarized FTIR-ATR spectra of the spin-coated films of **P1-3**, respectively. A ZnSe crystal was used for an internal reflection element (IRE). In these spectra, "$\theta = 90°$" and "$\theta = 0°$" represents the infrared light polarizing parallel and perpendicular to a substrate surface, respectively. Tentative assignments of the representative absorption peaks in these spectra are summarized in Table II. As for **P1**, each absorption peak intensity was independent of the polarized direction in the solid **B**, indicating that the mesogenic chromophores aligned randomly. On the other hand, the polarized direction dependence of each absorption peak intensity was observed in the solid **A**. When the polarized direction of the light was "$\theta = 0°$", the absorption peak intensities of the ring-stretching mode as well as the symmetric-stretching mode of the nitro group increased, while that of the asymmetric-stretching mode of the nitro group decreased.

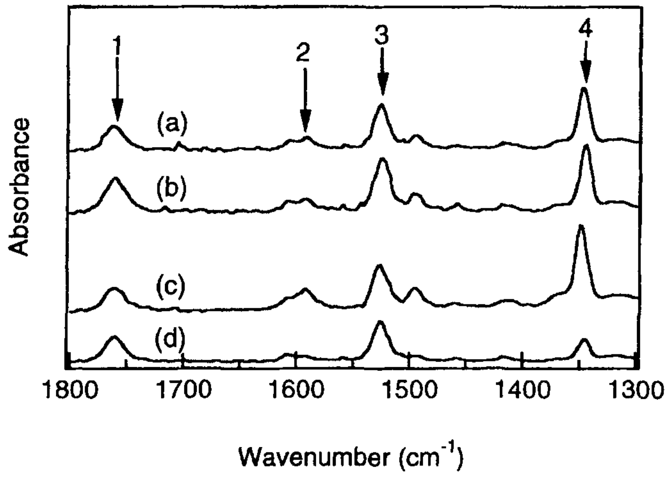

FIGURE 2 FTIR-ATR spectra of (a) solid **B** (θ = 0°), (b) solid **B** (θ = 90°), (c) solid **A** (θ = 0°) and (a) solid **A** (θ = 90°) of **P1** spin-coated film.

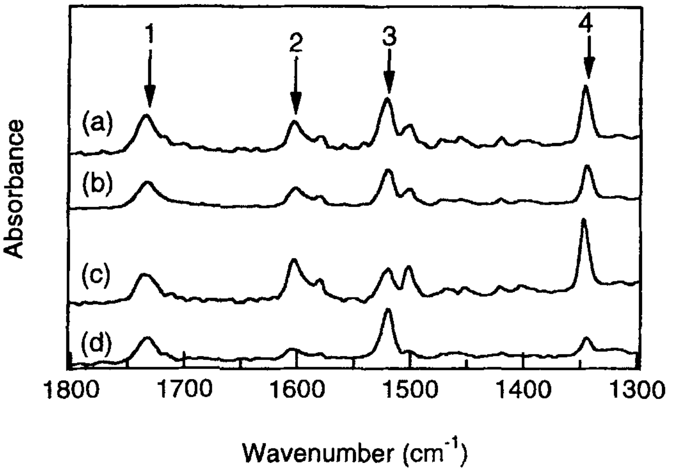

FIGURE 3 FTIR-ATR spectra of (a) solid **B** (θ = 0°), (b) solid **B** (θ = 90°), (c) solid **A** (θ = 0°) and (a) solid **A** (θ = 90°) of **P2** spin-coated film.

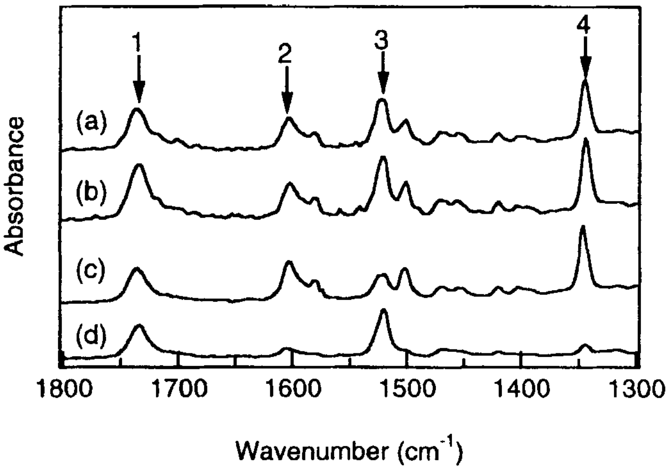

FIGURE 4 FTIR-ATR spectra of (a) solid **B** (θ = 0°), (b) solid **B** (θ = 90°), (c) solid **A** (θ = 0°) and (a) solid **A** (θ = 90°) of **P3** spin-coated film.

TABLE II Assignment of infrared absorption band of **P1**-**P3**

No.	wavenumber (cm^{-1})	assignment
1	1730	C=O stretch
2	1600	ring stretch
3	1520	NO_2 asymmetric stretch
4	1350	NO_2 symmetric stretch

On the contrary, when the polarized direction of the light was "θ = 90°", the absorption peak intensities of the ring-stretching mode and the symmetric-stretching mode of the nitro group reduced, while that of the asymmetric-stretching mode of the nitro group increased. These results suggest that the mesogenic chromophores of **P1** aligned almost perpendicular against a substrate surface in the solid **A**. The similar results could be obtained for the polarized FTIR-ATR spectra of **P2** and **P3**. Consequently, the alignment of the mesogenic chromophores of **P2** and **P3** is isotropic in the solid **B** and nearly perpendicular against a substrate surface in the solid **A**.

Determination of the Tilt Angle of the Mesogenic Chromophores in the Solid A by the Dichroic Ratio

In order to investigate the tilt angle from an orthogonal vector of a substrate surface to the mesogenic chromophores in the solid **A** of this polymer series, the dichroic ratios, R, were evaluated from the absorbance of the symmetric-stretching mode of the nitro group. The dichroic ratios could be calculated by the following equation,

$$R = A_{\parallel} / A_{\perp} = 2\cot^2\alpha$$

where α is the angle between the vibrational transition moment of the symmetric-stretching mode of the nitro group and the orthogonal vector of the substrate. $A_{\parallel}$ and $A_{\perp}$ indicate the absorbance at "$\theta = 0°$" and "$\theta = 90°$", respectively. However, the absolute intensity at "$\theta = 90°$" can not be compared directly with that at "$\theta = 0°$" because of the difference condition in the measurement. We normalized each FTIR-ATR spectrum by using the peak intensity of the absorption band of the stretching mode for the carbonyl group as a reference, since no dependence of the polarization angle on the absorbance of the stretching mode of the carbonyl group could be expected. Table III summarizes the tilt

TABLE III Tilt angles deduced from dichroic ratio in the solid **A**

polymer	methylene unit	tilt angle (deg)
P1	0	7.97
P2	6	12.8
P3	11	23.0

angles against a substrate surface deduced from the above analyses. As can be found in Table III, the tilt angle in the solid **A** clearly depends on the methylene spacer length. Further investigation for the effect of the spacer length on the tilt angle was conducted by the measurement of X-ray diffraction patterns.

Investigation of the Tilt Angle of the Mesogenic Chromophores by X-ray Diffraction Measurement

The X-ray diffraction patterns in the solid **A** and the smectic phase of **P1-3** are shown in Figure 5, which were measured by a powder method. A diffraction peak assigned to a layer spacing was clearly observed at a small-angle region on the diffraction pattern in the smectic phase of each polymer, and the values of the layer spacing are summarized in Table IV. The layer spacing increases linearly with the increase in the methylene units. These results indicate that the methylene units would form the trans conformation[21]. In addition, on the diffraction patterns in the solid **A** of these polymers, a diffraction peak assigned to a spacing of the π-stacking between the mesogenic chromophores was observed in a wide-angle region. Estimated separations between the mesogenic chromophores of **P1**, **P2** and **P3** are 3.64 Å, 3.54 Å and 3.54 Å, respectively. Thus, the spacing of the π-stacking between the mesogenic chromophores of **P1** is wider than those of other polymers. This result indicates that the intermolecular interaction between the mesogenic chromophores of **P1** is weak compared to those of other polymers.

TABLE IV Layer spacing and tilt angle deduced from X-ray diffraction patterns

polymer	layer spacing (Å)	tilt angle (deg)
P1	23.6	20.6
P2	34.5	35.4
P3	42.5	38.6

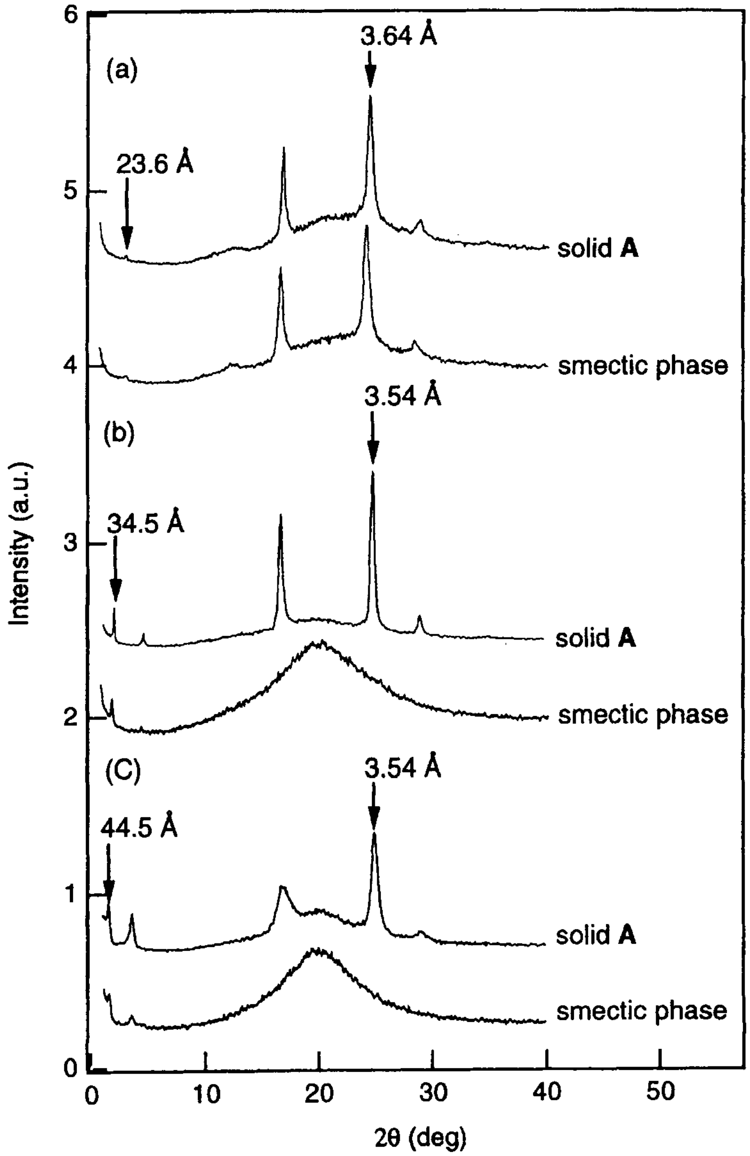

FIGURE 5 X-ray diffraction patterns of (a) **P1**, (b) **P2** and (c) **P3**.

Figure 6 shows the side-chain length of **P1-3** in their trans conformation. The side-chain length was estimated with the empirical molecular force field method. The mesogenic chromophores of these polymers would form the interdigitated alignment in the smectic phase as shown in Figure 7 due to the interactions of strong permanent dipole moment between the mesogenic chromophores. The tilt angles to an orthogonal vector of the layer plane were evaluated from the relation, $d = l \cos \theta$, in each smectic phase, where d is the layer spacing, l is the summation over side-chain length and the 4-nitro-substituted azobenzene chromophore. Deduced tilt angles are summarized in Table IV. It is found from Table IV that the tilt angle of the mesogenic chromophore in the smectic phase increases with the increase of the methylene units. Furthermore, these tilt angles in the smectic phase of each polymer are large compared to that in the solid **A**.

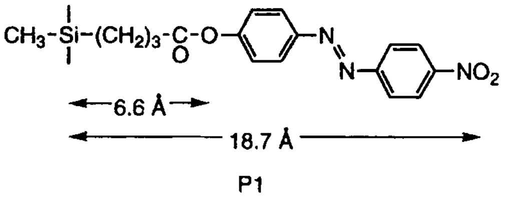

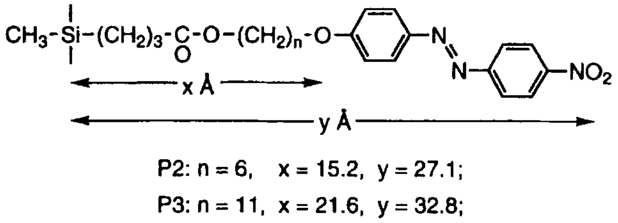

FIGURE 6 Side-chain length of **P1**, **P2** and **P3**.

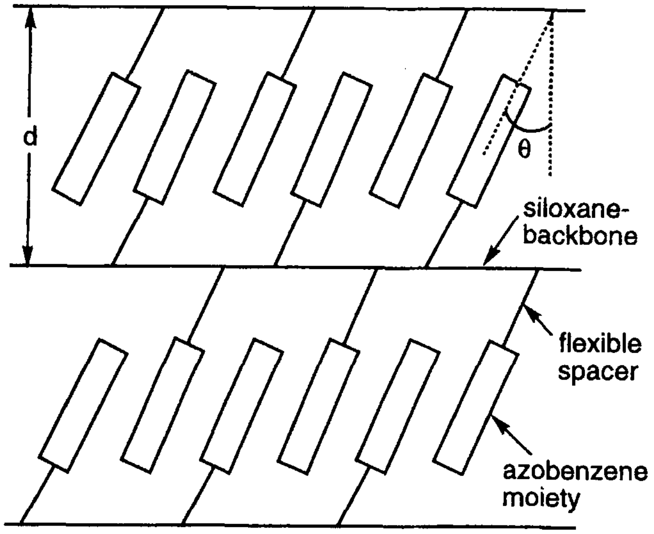

FIGURE 7 Schematic of packing manner of liquid-crystalline polysiloxanes used in this study.

UV-Vis Spectroscopy

In order to investigate the effects of the changes in the alignment of the mesogenic chromophores on the electronic state of the azobenzene moiety, the UV-Vis spectroscopy was measured in each phase of **P1-P3**. The intermolecular interactions acting on the mesogenic chromophores in the solid **A** could be known because the shape of the absorption spectrum was sensitive to the electrical interactions between the neighboring molecules. Figure 8 shows the temperature dependence of the UV-Vis absorption spectra of **P1**. These UV-Vis absorption spectra were measured by the transmission method for spin-coated films on a quartz substrate. There are significant differences between the spectra of the solid **A** and **B** for **P1**. The absorption band at ~340 nm can be assigned to the π–π* transition band of 4-nitro-substituted azobenzene. The electric dipole transition moment considered to be oriented nearly along the long axis of the azobenzene moiety[22]. Namely, the azobenzene moieties absorbs the light when its electric vector is parallel to the long axis of the azobenzene moieties.

Consequently, the differences in the absorbance at the absorption band ~340 nm can be attributable to the difference in the orientational direction of the mesogenic chromophores against the substrate. Thus, the mesogenic chromophores of **P1** aligned nearly perpendicular to the substrate surface in the solid **A**. Analyzing the relative absorbance of the absorption band, it can be considered that the tilt angle of the mesogenic chromophores against the substrate surface becomes greater accompanied with the transition from the solid **A** to the smectic and the nematic phases. This result is consistent with the result obtained by the FTIR-ATR spectra and the X-ray diffraction measurement. On the contrary, the mesogenic chromophores aligned at random in the isotropic phase and the solid **B**. The similar change was observed in the absorption spectra of **P2** and **3**. Namely, the phase transitions for **P2** and **3** are considered to induce the similar orientational behavior of the mesogenic chromophores as was found in **P1**. Moreover, splitting of the π–π^* transition band of the azobenzene moiety was observed in the solid **A** of **P2** and **P3**. The two chromophores can interact electrically with each other, and each of these almost identical chromophores will be perturbed by the electric transition dipole moment of the other in the excited state (exciton coupling), resulting in the splitting in energy of excited state (Davydov splitting)[23-25]. The splitting energy depend on the distance and angle between the two electric transition dipole moments of the chromophores. Consequently, such a splitting of the absorption band is originated in the exciton coupling between the mesogenic chromophores, and indicates that the strong electrical intermolecular interactions act between them in the solid **A** of **P2** and **P3**. On the other hand, the splitting of the π–π^* transition band of 4-nitro-substituted azobenzene was not observed in the absorption spectrum in the same state of **P1**. These results show that the electrical intermolecular interactions between the mesogenic chromophores of **P1** would be weak compared to those for **P2** and **P3**, and support the result of the X-ray diffraction measurement.

From the results of the UV-Vis spectroscopy and the X-ray diffraction measurement, the dependence of the intermolecular interactions on the spacer length was observed in the solid **A** of this series. Moreover, in the smectic phase, the interactions between the mesogenic chromophores would become also

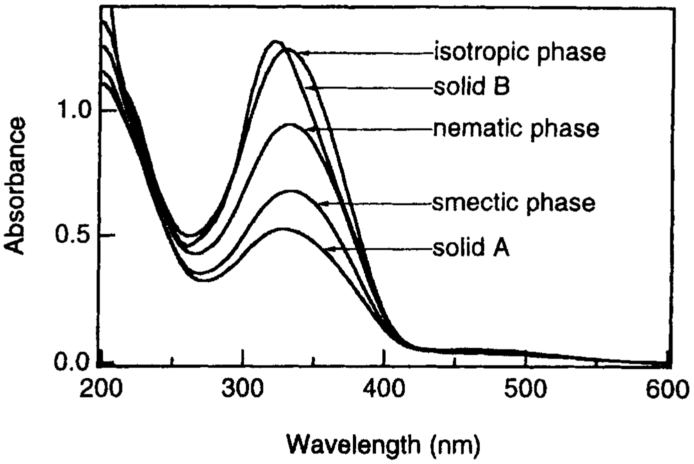

FIGURE 8 UV-Vis absorption spectra of **P1** spin-coated film.

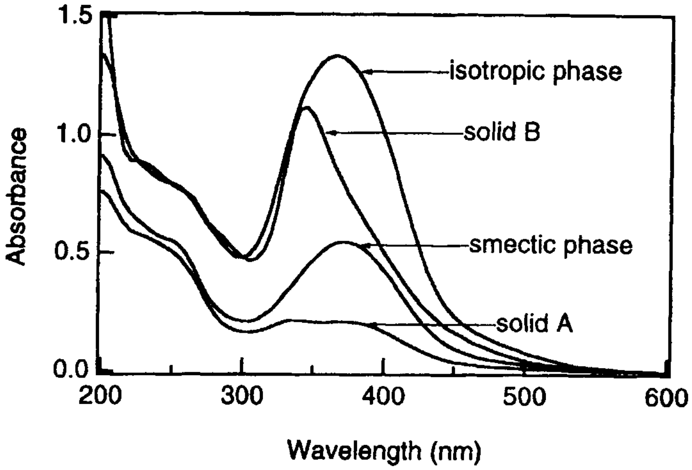

FIGURE 9 UV-Vis absorption spectra of **P2** spin-coated film.

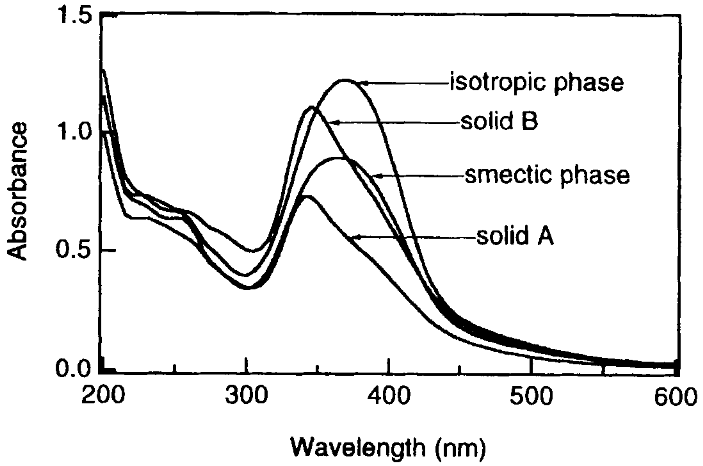

FIGURE 10 UV-Vis absorption spectra of **P3** spin-coated film.

more strong with the increase of the methylene units because the temperature range of the smectic phase depend on the spacer length, as shown in Table I. Such a spacer length dependence of the intermolecular interactions would be due to the improvement of the mobility of the side chain with the increase of the methylene units. Furthermore, it would be considered that the mesogenic chromophores of this series tilt in order to form the more stable packing structure in the smectic and the solid A.

CONCLUSION

The orientational behavior in the different phase structure and the influence of spacer length on the tilt angle of the mesogenic chromophores were investigated using three kinds of side-chain liquid-crystalline polysiloxanes which have different spacer length. From the UV-Vis, polarized FTIR-ATR spectroscopy and X-ray diffraction measurements, the mesogenic chromophores of these polymers in the smectic phase and the solid **A** were found to align spontaneously nearly normal to the substrate. The tilt angle from the orthogonal vector of the substrate of the mesogenic chromophores becomes smaller in the solid **A** compared with the smectic phase. Moreover, when the polymer exhibits the nematic phase, the tilt angle of the mesogenic chromophores was found to be greater than that in the smectic phase. The tilt angles of the mesogenic chromophores of these polymers in the smectic phase and the solid **A** increased with the increase in the side-chain methylene units. The dependence of the tilt angle on the spacer length was concluded to be attributable to the changes of the intermolecular interactions with relation to the degree of the motion decoupling between the side-chain and main-chain.

References

[1.] H. Finkelmann; G. Rehage, *Makromol. Chem. Rapid. Commun.*, **1**, 733 (1980).
[2.] R. V. Tarlose; V. Sinitzyn; V. P. Shibaev; N. A. Plate, *Mol. Cryst. Liq. Cryst.*, **80**, 211 (1982).
[3.] K. H. Wassemer; E. K. Ohmes; G. Kothe; M. Portugall; H. Ringsdorf, *Makromol. Chem., Rapid Commun.*, **3**, 281 (1982).
[4.] W. M. K. P. Wijekoon; Y. Zhang; S. P. Karna,; P. N. Prasad; A. C. Griffin; A. M. Bhatti, *J. Opt. Soc. Am. B.*, **9**, 1832 (1992).
[5.] M. Eich; J. H. Wendorff, *Makromol. Chem. Rapid. Commun.*, **8**, 467 (1987).
[6.] T. Ikeda; O. Tsutsumi, *Science*, **268**, 1873 (1995).
[7.] N. A. Platé, *Liquid-Crystal Polymers* (Plenum Press, New York, 1993), p. 213.
[8.] H. Finkelmann; M. Happ; M. Portugall; H. Ringsdorf, *Makromol. Chem.*, **179**, 2541 (1978).
[9.] H. Finkelmann; G. Rehage, *In Liquid Crystal Polymers 2/3 Advances in Polymer Science 60/61* (Springer-Verlag: West Berlin, 1984), p. 99.
[10.] R. Simon; H. J. Coles, *Polymer*, **27**, 811 (1986).
[11.] H. Finkelmann; J. Koldehoff; H. Ringsdorf, *Angew. Chem. Int. Ed. Engl.*, **17**, 935 (1978).
[12.] V. P. Shibaev; V. M. Moiseenko; Y. S. Freidzon; N. A. Platé, *Eur. Polym. J.*, **16**, 2777 (1980).
[13.] V. P. Shibaev; S. G. Kostromin; N. A. Platé, *Eur. Polym. J.*, **18**, 651 (1982).
[14.] Y. S. Freidzon; A. V. Kharitonov; V. P. Shibaev; N. A. Platé, *Eur. Polym. J.*, **21**, 211 (1985).
[15.] S. G. Kostromin; V. V. Sinitzyn; R. V. Talroze; V. P. Shibaev; N. A. Platé, *Makromol Chem. Rapid. Commun.*, **3**, 809 (1982).
[16.] T. Yamaguchi; T. Asada; H. Hayashi; N. Nakamura, *Macromolecules*,

22, 1141 (1989).
[17.] N. A. Platé; V. P. Shivaev, *Comb-Shaped Polymers and Liquid Crystals* (Plenum Press, New York, 1987).
[18.] S. Kurihara; T. Ikeda; S. Tazuke, *Macromolecules*, **26**, 1590 (1993).
[19.] N. Nemoto; Y. Nagase; J. Abe; H. Matsushima; Y. Shirai, *Macromol. Chem. Phys.*, **196**, 2237 (1995).
[20.] J. Abe; M. Hasegawa; H. Matsushima; Y. Shirai; N. Nemoto; Y. Nagase, *Macromolecules*, **28**, 2938 (1995).
[21.] K. Berger; M. Ballauff, *Mol. Cryst. Liq. Cryst.*, **157**, 109 (1988).
[22.] H. Bisle; M. Romer; H. Rau, *Ber. Bunsenges. Phys. Chem.*, **80**, 301 (1976).
[23.] A. S. Davydov, *Theory of Molecular Excitons* (McGraw-Hill, New York, 1962).
[24.] A. S. Davydov, *Phys, Status Solidi*, **20**, 143 (1967).
[25.] A. S. Davydov, *Theory of Molecular Excitons* (Plenum Press, New York, 1971).